Adam D. Rosenthal
Massachusetts Institute of Technology,
Department of Electrical Engineering and Computer Science,
Laboratory for Electromagnetic and Electronic Systems
Cambridge, MA 02139

Carlos Rinaldi
Massachusetts Institute of Technology,
Department of Chemical Engineering
Cambridge, MA 02139

Thomas Franklin

Markus Zahn

Massachusetts Institute of Technology,
Department of Electrical Engineering and Computer Science,
Laboratory for Electromagnetic and Electronic Systems
Cambridge, MA 02139

Torque Measurements in Spin-Up Flow of Ferrofluids

Measurements of magnetic-field-induced torque in applied uniform rotating magnetic fields are presented and compared to theoretical analyses for water- and oil-based ferrofluids. These experiments measure the viscous torque on the inner wall of a stationary hollow polycarbonate spindle that is completely filled with ferrofluid and attached to a viscometer functioning as a torque meter. The spindle remains stationary and is centered inside a three-phase AC 2-pole motor stator winding, creating uniform time-varying rotating magnetic fields. The viscous torque is measured as a function of magnetic field amplitude, frequency, and direction of rotation. These measurements demonstrate that ferrofluid flow and torque are present even in the absence of free surfaces and agree with a recently derived analysis of the torque during spin-up flow of ferrofluids.
[DOI: 10.1115/1.1669030]

1 Introduction

Ferrofluids [1] are suspensions of permanently magnetized colloidal particles coated by a stabilizing dispersant and immersed in a suitably chosen carrier fluid. In the presence of time-varying magnetic fields, ferrofluid particles will rotate in order to align their magnetic dipole moment with the applied field. However, because of the fluid viscosity, the magnetization $\mathbf{M}$ will lag behind the time-varying magnetic field $\mathbf{H}$, thereby resulting in a body-torque density on the ferrofluid, given by $\mu_0\mathbf{M}\times\mathbf{H}$ (with $\mu_0 = 4\pi\times10^{-7}$ Henries/m the magnetic permeability of free space), which causes fluid flow. In our experiments, the viscous torque from this magnetic-field-induced flow is measured using a Couette viscometer, as a function of magnetic field amplitude and frequency.

Ferrofluids are a scientifically and commercially important realization of polarizable systems. As such, they are characterized by the presence and effect of long-range body-couples and nonsymmetric viscous stresses, as well as more exotic phenomena, such as couple stresses representing the direct-contact transport of microstructure angular momentum. Due to their physical, chemical, and magnetic properties, ferrofluids are of increasing interest in the design of magneto-responsive colloidal extractants [2], microfluidic pumps and actuators driven by alternating or rotating magnetic fields [3–7], and in biological/biomedical applications such as drug delivery vectors, magnetic cell sorting schemes, and magnetocytolysis treatment of localized tumors [8,9].

The phenomenon of spin-up flow of ferrofluids has received considerable attention [10–15] during the development of the field of ferrohydrodynamics. Experiments are carried out by placing a sample of ferrofluid in an open-top cylindrical container subjected to a rotating magnetic field. In such a stationary cylindrical container, the top surface of the ferrofluid is observed to rotate rigid-body-like in a direction which depends on the applied magnetic field amplitude and frequency. Such essentially rigid-body motion is observed at the top free surface of the fluid right out to the stationary cylindrical vessel wall, except for a thin boundary layer.

The general perception in the literature is that the ferrofluid and magnetic field rotate in opposite directions. However, some authors [11–13] report observations where the ferrofluid switches between co-rotation and counter-rotation with respect to the applied magnetic field depending on magnetic field amplitude and frequency. Explicitly, [12] reports co-rotation of field and fluid for low applied fields and counter-rotation for high applied magnetic fields, whereas [11] and [13] observe counter-rotation for low applied magnetic fields and co-rotation for higher applied fields. We have made similar observations in our laboratory, where a water-based ferrofluid placed in a cylindrical container and subjected to the uniform rotating magnetic field generated by a three-phase two-pole magnetic machine stator winding is observed to co-rotate with the applied magnetic field for small magnetic fields and counter-rotate with respect to the magnetic field for large magnetic fields. In addition to this, we have observed the direction of free-surface rotation change depending on the axial location of the free surface in the gap of the magnetic machine stator.

The confusion regarding field and fluid rotation sense, and the applicability of various theoretical analyses [16–20], is compounded when one considers that all available observations are made at the free-surface of the opaque ferrofluid using various types of tracer beads, with no way to determine the flow profiles prevailing throughout the volume of fluid. It is clear that surface flow observations will be problematic and probably not representative of the bulk-flow situation when one considers that curvature-driven flows have been observed at ferrofluid free surfaces [15]. Thus, there remains a need for accurate, direct measurements of bulk-flow related quantities. One such quantity is the total torque required to restrain the hollow cylinder containing the ferrofluid.

Observations of counter-rotation of field and fluid led [11] to investigate the direction in which the cylindrical container would rotate if it could freely do so. This represents an indirect measurement of the magnetic torque applied on the ferrofluid. One would expect the counter-rotating fluid to drag the cylindrical container with it, but experiments show the container co-rotating with the field whereas the fluid counter-rotates. Such observations have

Contributed by the Fluids Engineering Division for publication in the JOURNAL OF FLUIDS ENGINEERING. Manuscript received by the Fluids Engineering Division January 17, 2003; revised manuscript received June 14, 2003. Associate Editor: D. Siginer

Table 1 Physical and magnetic properties at room temperature for water-based and Isopar-M ferrofluids used

Ferrofluid	ρ, [kg/m^3]	η, [Nsm^{-2}]	$\mu_0 M_s$, † [Gauss]	$\phi^\ddagger$	χ^*
Water-based	1,220	0.007	203	0.036	0.65
Isopar-M	1,180	0.011	444	0.079	2.18

†Determined using equation (5).
‡Determined using equation (4).
*Determined using Fig. 2.

since been corroborated by [12] and [15]. However, all these observations are of a qualitative nature, not having directly measured the actual torque required to restrain the container. Hence, the motivation of our contribution—to obtain direct quantitative measurements of the torque required to restrain the cylindrical container during spin-up flow of a ferrofluid.

2 Ferrofluid Material and Magnetic Properties

Two types of ferrofluid were obtained from Ferrofluidics Corporation (Nashua, NH): a water-based ferrofluid (MSGW11) and an oil-based ferrofluid with Isopar-M as the carrier fluid (NF1634), each with ~10 nm diameter magnetite particles. Ferrofluid density ρ, viscosity η, and magnetization curves were measured. From the magnetization curves the saturation magnetization $\mu_0 M_s$, volume fraction of magnetic particles ϕ, magnetic susceptibility χ, magnetic particle diameter d, and magnetic time constants (τ_B, τ_N, τ) were determined for both ferrofluids. These results are summarized in Tables 1 and 2.

Physical Properties. The ferrofluid densities were determined gravimetrically using an analytical mass balance and a calibrated burette. The shear viscosity η for each ferrofluid at zero applied magnetic field was measured at room temperature using a Brookfield viscometer Model LVDV-I+. The recommended Brookfield procedure was used, using 500 mL of ferrofluid in a 600 mL beaker and the Brookfield calibrated stainless steel spindle LV1. The resulting values of density and viscosity are shown in Table 1.

Magnetization Characteristics

Demagnetizing Factor. In determining the magnetic properties of the ferrofluid, it is important to differentiate between the externally applied magnetic field and the magnetic field inside the ferrofluid. The difference between the external magnetic field $\mathbf{H}_e$ and the internal magnetic field $\mathbf{H}_i$ is described by the demagnetization factor, D, given by

$$\mathbf{H}_i = \mathbf{H}_e - \mathbf{M}D. \tag{1}$$

The demagnetization field arises due to effective magnetic charge induced on the surface of a magnetic material with magnetization $\mathbf{M}$, which partially cancels the externally applied magnetic field. Magnetization curves of the ferrofluids were measured using a

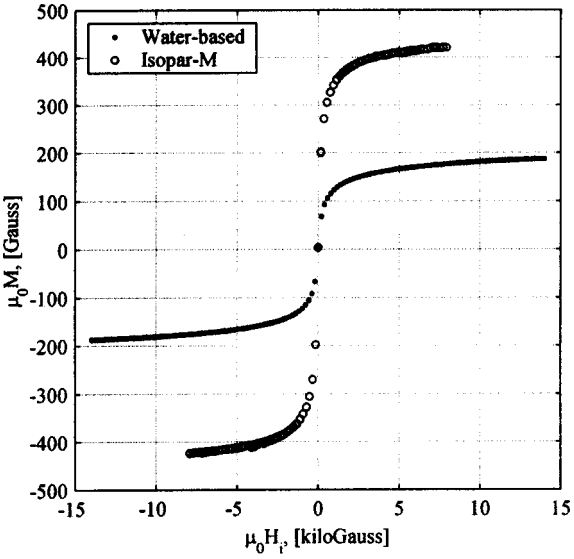

Fig. 1 Magnetization curves for water-based and Isopar-M ferrofluids obtained using a DMS Vibrating Sample Magnetometer at room temperature, $T = 299$ K

Digital Measurement Systems (DMS) Vibrating Sample Magnetometer Model 880. Ferrofluid samples were placed in the DMS plastic sample containers, whose dimensions approximate those of an oblate ellipsoid with major to minor axis ratio of $n = 2.4$. The demagnetizing factor D corresponding to an oblate ellipsoid is [21]

$$D = \frac{1}{2}\left[\frac{n^2}{(n^2-1)^{3/2}}\arcsin\frac{\sqrt{n^2-1}}{n} - \frac{1}{n^2-1}\right]. \tag{2}$$

Using (2) and $n = 2.4$ we obtain a demagnetization factor of $D = 0.211$. This value and (1) were used to calculate the internal magnetic field used in the abscissa of the magnetization curves shown in Figs. 1 and 2. This correction is especially important at low magnetic fields, shown in Fig. 2, where the low field magnetic susceptibility is determined.

Saturation Magnetization. For a monodisperse ferrofluid the Langevin equation describes the equilibrium magnetization for a given applied magnetic field [1]:

$$\frac{M}{M_s} = L(\alpha) = \coth\alpha - \frac{1}{\alpha}, \tag{3}$$

where $\alpha = M_d V_p \mu_0 H_i / kT$, with $V_p = \pi d^3/6$ the magnetic core volume per particle. The magnetic volume fraction is defined as

$$\phi = \frac{M_s}{M_d}, \tag{4}$$

Table 2 Estimated magnetic particle diameters and relaxation times at room temperature for water-based and Isopar-M ferrofluids used

Ferrofluid	$d_{\min}$, [nm]†	$d_{\max}$, [nm]‡	$d_{\max}$, [nm]*	τ_B, [s]**	τ_N, [s]§	τ, [s]$^+$
Water-based	5.5	11.9	11.4	2×10^{-6}–10^{-5}	5×10^{-9}–2×10^{-2}	5×10^{-9}–1×10^{-5}
Isopar-M	7.7	13.8	12.6	7×10^{-6}–2×10^{-5}	10^{-7}–200	10^{-7}–2×10^{-5}

†Determined using Eq. (5).
‡Determined using Eq. (6).
*Determined using Eq. (7).
**Determined using Eq. (9) and assuming 2 nm surfactant bi-layer thickness [2].
§Determined using Eq. (10).
$^+$Determined using Eq. (11).

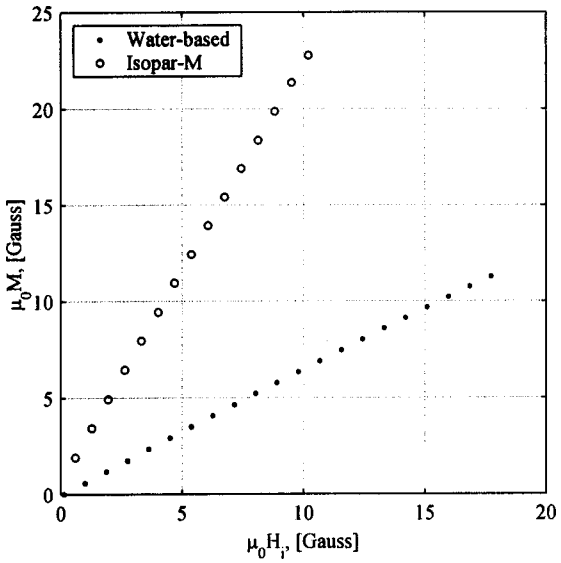

Fig. 2 Linear region (low-field) of the magnetization curves obtained for water-based and Isopar-M ferrofluids at room temperature, T=299 K

where M_d is the domain magnetization ($=446$ kAm^{-1} for magnetite). Obtaining a value of M_s is difficult experimentally since it requires application of a magnetic field of infinite magnitude. Yet ϕ can be calculated from (4) and the high-applied-field asymptote of the Langevin curve [1]:

$$\lim_{\alpha \gg 1} L(\alpha) \approx \left(1 - \frac{1}{\alpha}\right) = \left(1 - \frac{6}{\pi} \frac{kT}{\mu_0 M_d H_i d^3}\right), \tag{5}$$

where T is the absolute temperature, and $k = 1.38 \times 10^{-23}$ J/K is Boltzmann's constant. Equation (5) is a linear relationship between M and $1/H_i$ and can be rewritten as $\mu_0 M = c + b/(\mu_0 H_i)$ where $c = \mu_0 M_s$ and $b = -6kT\mu_0 M_s/(\pi M_d d^3)$. The parameters b and c are determined by a least-squares fit to the measurements of Fig. 1 in the high field region where $\alpha \gg 1$ to yield estimated values for the saturation magnetization and particle diameter for the smallest magnetic particles. In our study, we fit the uppermost and lowermost 30 data points (60 in total).

Magnetic Susceptibility. In order to determine the initial magnetic susceptibility, the slope of the low-field linear region was determined. The magnetization curves in Fig. 1 do not have enough precision in the low-field region to accurately determine the slope. For this reason, the low-field linear region was separately measured for the water-based ferrofluid and the Isopar-M ferrofluid and is shown in Fig. 2. The slope, corresponding to the initial magnetic susceptibility $\chi = M/H$, was determined through a simple linear least-squares fit of the data and is listed in Table 1.

Magnetic Particle Size. Ferrofluids are expected to have a range of particle sizes that can be determined by examination of the magnetization behavior. The minimum particle diameter was estimated from the high-field asymptote of the Langevin curve, by rearranging the coefficient b of the linear fit for d. Since the coefficient b is most affected by the smallest particles, this calculation provides an estimate for the minimum particle diameter $d = d_{\min}$.

The maximum particle diameter for the water-based ferrofluid was estimated by using the low-field limit of the Langevin curve [1]:

$$\lim_{\alpha \ll 1} L(\alpha) \approx \frac{\alpha}{3} = \frac{\pi}{18} \frac{\mu_0 M_d H_i d^3}{kT}, \tag{6}$$

and the value of the initial susceptibility, $\chi = \alpha M_S/(3H_i)$, obtained from the slope of Fig. 2. Here, α is most affected by the larger particles, thus providing an estimate for the maximum magnetic particle diameter.

For suspensions that are non-dilute with respect to the magnetic cores Shliomis [22] gives a correction to (6) using the Debye-Onsager theory of polar fluids [23] to account for the effect of dipole-dipole interactions

$$\frac{\chi(2\chi+3)}{\chi+1} = \frac{\pi}{6} \phi \frac{\mu_0 M_d^2 d^3}{kT}. \tag{7}$$

The resulting particle diameter ranges thus obtained are summarized in Table 2, with values given for minimum diameter using (5) and maximum diameter using (6) and (7). Note that these diameters are only estimates. Direct experimental observation shows that the actual diameter of the magnetic particle cores may be as much as 2 nm larger than the estimates obtained from the Langevin relation [2].

Relaxation Times. In studying the dynamics of ferrofluids in time-varying magnetic fields, one must consider how the local magnetization changes, or "relaxes," due to fluid convection, particle rotation, and applied fields. The commonly accepted magnetic relaxation equation for an incompressible, magnetically linear ferrofluid undergoing simultaneous magnetization and reorientation due to fluid convection at flow velocity $\mathbf{v}$ and spin angular velocity $\boldsymbol{\omega}$ is [1,24]:

$$\frac{\partial \mathbf{M}}{\partial t} + \mathbf{v} \cdot \nabla \mathbf{M} - \boldsymbol{\omega} \times \mathbf{M} - \frac{1}{\tau}[\mathbf{M} - \chi \mathbf{H}] = 0, \tag{8}$$

where τ is the effective relaxation time constant. Equation (8) is applicable under conditions not far removed from magnetization equilibrium [25–27].

The two commonly accepted mechanisms by which ferrofluid magnetic particles relax are Brownian motion, resulting from collision between the magnetic particle and the constituent molecules of the suspending medium, and Néel relaxation, resulting from rearrangement of the magnetic domains without rotation of the particle. The characteristic time describing Brownian motion is [1]

$$\tau_B = \frac{4\pi\eta_0 R^3}{kT}, \tag{9}$$

where η_0 is the shear viscosity of the suspending fluid, and $R = R_p + \delta$ is the hydrodynamic radius, i.e. the sum of the magnetic particle radius, $R_p = d/2$, and the surfactant layer thickness, δ. In estimating the Brownian relaxation time we have assumed the surfactant layer thickness δ is approximately 2 nm [2].

The Néel relaxation time is given as [1]

$$\tau_N = \frac{1}{f_0} e^{(kV_p/kT)}, \tag{10}$$

where f_0 is a characteristic frequency of the magnetic material ($=10^9$ Hz for magnetite), and K is the anisotropy constant of the magnetic domains. The literature gives different values for the anisotropy constant of magnetite, over the range of 23,000 to 100,000 Joules/m^3. Recent work [28] has used Mossbauer spectroscopy to show that the value of K is size dependent, increasing as particle size decreases and gives a value of $K = 78{,}000$ Joules/m^3 for 12.6 nm diameter magnetite nanoparticles, which is the value we use in estimating values of τ_N in this work.

The two relaxation processes described above occur in parallel and therefore the effective time constant describing magnetic particle relaxation is given by

$$\frac{1}{\tau} = \frac{1}{\tau_B} + \frac{1}{\tau_N} \Rightarrow \tau = \frac{\tau_B \tau_N}{\tau_B + \tau_N}. \tag{11}$$

The estimated ranges of the resulting Brownian, Néel, and effective relaxation times thus obtained are summarized in Table 2

based on the estimated range of particle size using (5)–(7). Note that the calculated Néel relaxation times vary by seven orders of magnitude for the estimated particle sizes of water-based ferrofluid and by nine orders of magnitude for the Isopar-M ferrofluid, thus, direct experimental determination would be preferable and will be the subject of future work.

3 Apparatus and Experimental Method

We have used a Brookfield Model LVDV-I+ viscometer as a torque meter. When a fixed rotation speed is selected the spindle rotates counterclockwise as the viscometer applies the necessary torque to keep it rotating at the specified speed. When the magnetic-field-induced shear stress on the spindle is in the clockwise direction, i.e. in the direction opposite to spindle rotation, it is harder to turn the spindle at the specified speed; therefore the viscometer applies a higher torque, larger than the torque required to shear the fluid in the absence of a magnetic field. On the other hand, when the magnetic-field-induced shear stress on the spindle is in the counterclockwise direction, i.e. in the same direction as spindle rotation, it is easier to rotate the spindle at the specified speed; therefore the viscometer applies a lower torque, as compared to the torque required to shear the fluid in the absence of a magnetic field.

For our experiments the spindle was set to remain stationary, hence, with zero applied magnetic field no torque is required from the viscometer to restrain the spindle. Under conditions for which a clockwise magnetic-field-induced shear stress arises, a positive torque will be registered, whereas for a counterclockwise shear stress a negative torque will be measured. The range of measurable torque for our Brookfield viscometer is -6.73 μN-m to $+67.3$ μN-m.

The hollow Lexan® (polycarbonate) spindle used in these experiments was completely filled with ferrofluid. The spindle has an inner diameter of 19.6 mm and a hollow chamber length of 62.4 mm, yielding a total volume of 18.8 mm^3. It is important that the spindle be non-conducting and non-magnetic so that the measured torque on the spindle is entirely due to ferrofluid shear stress. The standard stainless steel spindle would act like an induction motor in a time varying magnetic field due to induced eddy currents, which would cause additional magnetic torque on the spindle and thus confuse separation of ferrofluid viscous torque from induction motor torque.

The plastic spindle was placed so that the fluid is centered along the axis of the three phase, 2-pole motor stator winding (uniform magnetic field source in the absence of ferrofluid) with inner bore of 78 mm diameter and magnetic core height 63 mm. The magnetic fields in the motor stator winding were generated using sinusoidally time varying currents with the appropriate phase differences to create magnetic fields that rotate clockwise or counterclockwise.

Measurements were taken at frequencies of 5, 10, 50, 100, 500, 1,000, 2,000, and 5,000 Hz with an input current of 0, 1, 2, 3, 4, and 5 Amps peak. In the 2-pole stator, each ampere of peak input current corresponds to a uniform external magnetic field of 26 Gauss rms. These magnetic field measurements were made in the absence of ferrofluid, and therefore reflect the external magnetic field and do not incorporate the demagnetizing effect of the ferrofluid. Over the space occupied by the ferrofluid filled spindle, the external magnetic field increased from the radial center of the winding by less than 2% at 10 mm radius with negligible variation over angle from zero to 360 degrees. In the axial direction the magnetic field decreased from the axial center of the winding by less than 18% at the top and bottom of the iron core of the winding, 31.2 mm above and below the axial center of the winding.

For higher frequencies, some trials contain fewer data points. This is either because the torque was outside the maximum operating torque range for the Brookfield viscometer or because the voltage across the motor winding terminals was too high for safe operation. With an applied current at frequency f, the inductive reactance $L\Omega_f$ increases with radian frequency $\Omega_f = 2\pi f$ and limits the current that can be supplied to the stator winding. By adding the appropriate capacitor, C, in series with the motor, a resonant circuit was used so the capacitive reactance $1/[C\Omega_f]$ cancels the inductive reactance, i.e. $L\Omega_f = 1/[C\Omega_f]$, thereby decreasing the high frequency winding impedance so that 1 to 5 ampere currents could be applied. This modification to the experimental setup was needed at frequencies of 500 Hz and above.

4 Measurements of Torque During Spin-Up Flow

Figures 3 and 4 present the measured torque vs. magnetic field amplitude for various frequencies with clockwise magnetic field rotation in the range of 5 Hz–5 kHz. The spindle remained stationary for all measurements. Measurements were performed for both clockwise and counter-clockwise magnetic field rotation, for which the torque just reverses sign. Thus, we mainly present data here for clockwise magnetic field rotation as this results in a clockwise viscometer torque for which our viscometer had the largest operating range.

The torque required to restrain the spindle was measured as a function of magnetic field amplitude for the water-based ferrofluid and Isopar-M ferrofluid as shown in Fig. 3. Both measurement sets show that the measured torque, and therefore the magnetic-field-induced shear stress, increases with magnetic field amplitude. The measured torque also increases with the applied field frequency, particularly for the Isopar-M ferrofluid. For the water-based ferrofluid the torque is seen to scale with applied frequency for the lower frequencies but apparently this dependence saturates at the higher field frequencies.

The data of Fig. 3 is re-plotted in Fig. 4, now with torque as a function of applied-field frequency. Both figures show that the measured torque increases with magnetic field frequency, except for the water-based ferrofluid at frequencies of 500 Hz and above, which show torque saturation with respect to field frequency f.

5 Analysis of Torque on the Hollow Spindle

The torque on the internal wall of the hollow spindle potentially has two components: (i) the torque due to surface-excess magnetic forces stemming from the rapid change in magnetic properties at the wall-fluid interface, and (ii) the torque due to viscous traction and the action of the magnetic fluid's couple-stress pseudodyadic. In general, both must be accounted for when deriving expressions for the experimental torque applied to restrain the stationary hollow spindle.

5.1 Surface-Excess Magnetic Torque. The surface-excess magnetic torque at the wall-fluid interface may be conveniently obtained by evaluating the jump in the ''magnetic stress'' tensor (or the so-called Maxwell stress) across the wall-fluid interface. Use of this mathematical technique circumvents the need to know the exact distribution of magnetic fields in this region with rapidly varying magnetic properties. The Maxwell stress applicable to an incompressible ferrofluid is given by [1,29]

$$\mathbf{T}^M = \mathbf{BH} - \frac{1}{2}\mu_0 H^2 \mathbf{I}; \quad \mathbf{B} = \mu_0(\mathbf{H}+\mathbf{M}) \tag{12}$$

where $\mathbf{I}$ is the identity tensor.

We are interested in determining the θ-directed shear stress component due to the jump in the Maxwell stress tensor across the ferrofluid-spindle wall interface (the r-directed component is of no consequence as it does not contribute to the z-directed torque, which is the experimentally measurable quantity). The θ-directed surface-excess magnetic force per unit area on the cylindrical wall at radius R, f_θ^M, is given by the jump in the $r\theta$-component of the Maxwell stress

$$\begin{aligned} f_\theta^M &= T_{r\theta}^M(r=R^+) - T_{r\theta}^M(r=R^-), \\ &= (B_r H_\theta)|_{r=R^+} - (B_r H_\theta)|_{r=R^-}. \end{aligned} \tag{13}$$

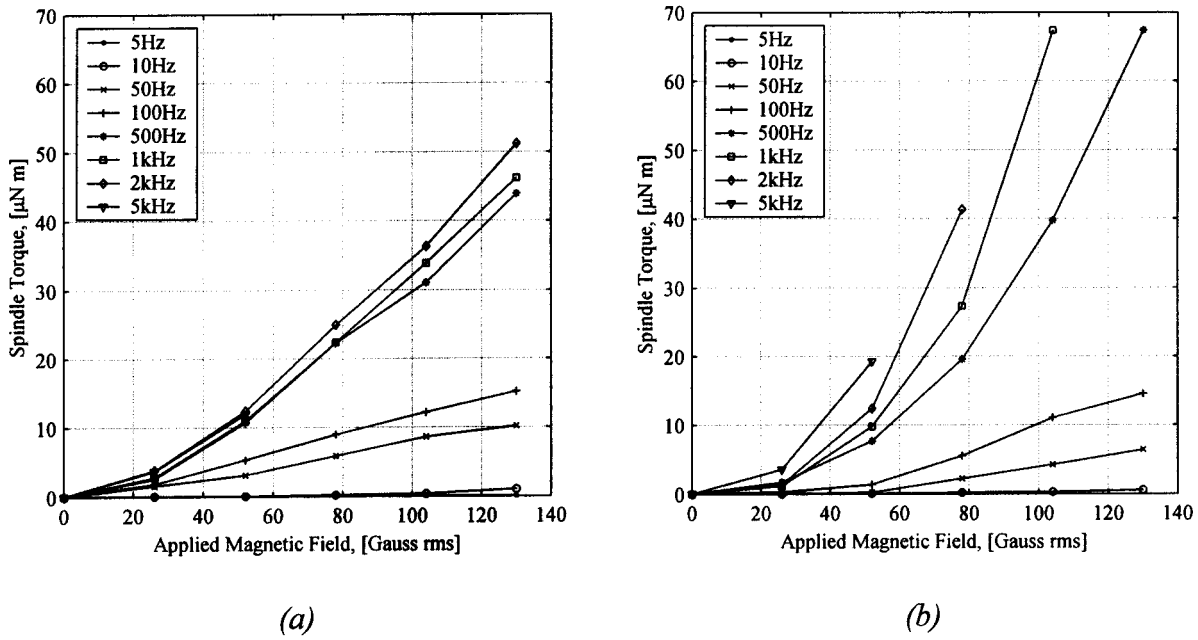

Fig. 3 Torque required to restrain the ferrofluid-filled plastic spindle as a function of magnetic field amplitude at various frequencies for the (*a*) water-based and (*b*) Isopar-M ferrofluids in a clockwise rotating uniform magnetic field generated by a two-pole induction motor stator winding. Interpolating lines have been added to aid the reader in distinguishing trends in the data

However, the jump conditions on the magnetoquasistatic field require that the normal component of $\mathbf{B}(\mathbf{x})$, B_r, and the tangential component of $\mathbf{H}(\mathbf{x})$, H_θ, be continuous across the wall-fluid interface, therefore, no surface-excess magnetic force results in the azimuthal direction

$$f_\theta^M = 0. \tag{14}$$

Because there is no surface-excess magnetic force in the azimuthal direction, there is no surface-excess magnetic torque on the cylindrical container wall.

5.2 Viscous Torque and Couple Stress. The torque on the spindle wall due to ferrofluid flow immediately proximate to it arises through two contributions: (i) the torque arising due to the viscous traction on the wall, and (ii) the torque due to gradients in particle spin, embodied in the couple-stress pseudodyadic $\mathbf{C}$. The first contribution is that familiar to fluid mechanics and arises due to the Cauchy stress $\mathbf{T}$ in the suspension, albeit modified to account for antisymmetric stresses. The second is an additional contribution due to the structured continuum nature of the ferrofluid

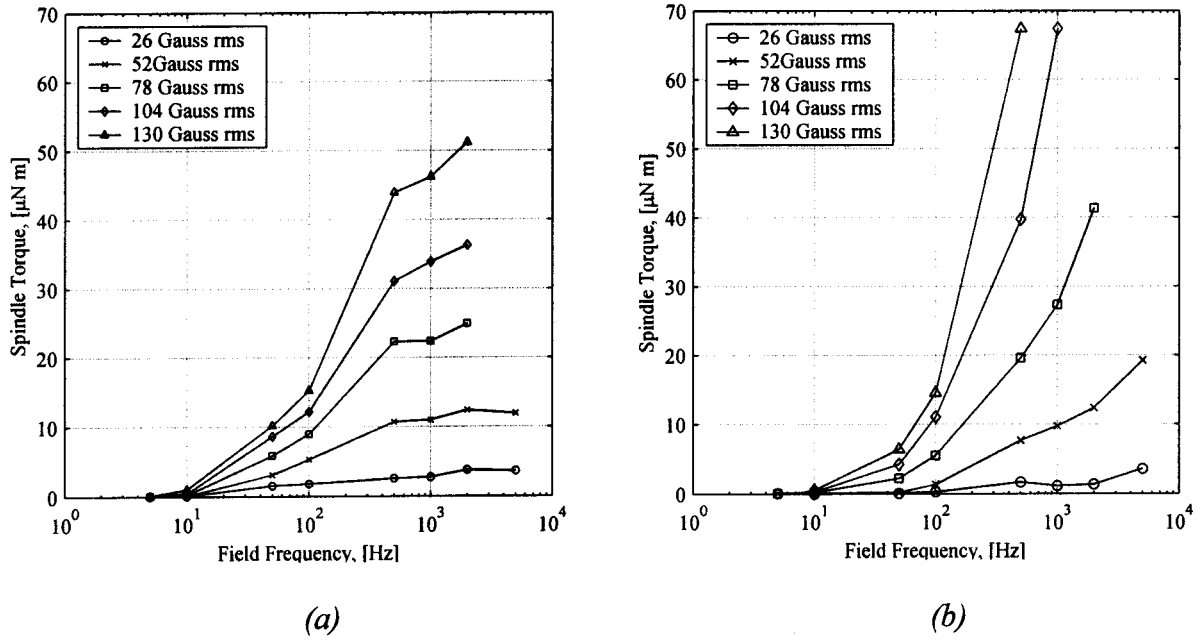

Fig. 4 Re-plot of Fig. 3 torque data as a function of magnetic field frequency at various magnetic field amplitudes for (*a*) water-based and (*b*) Isopar-M ferrofluids

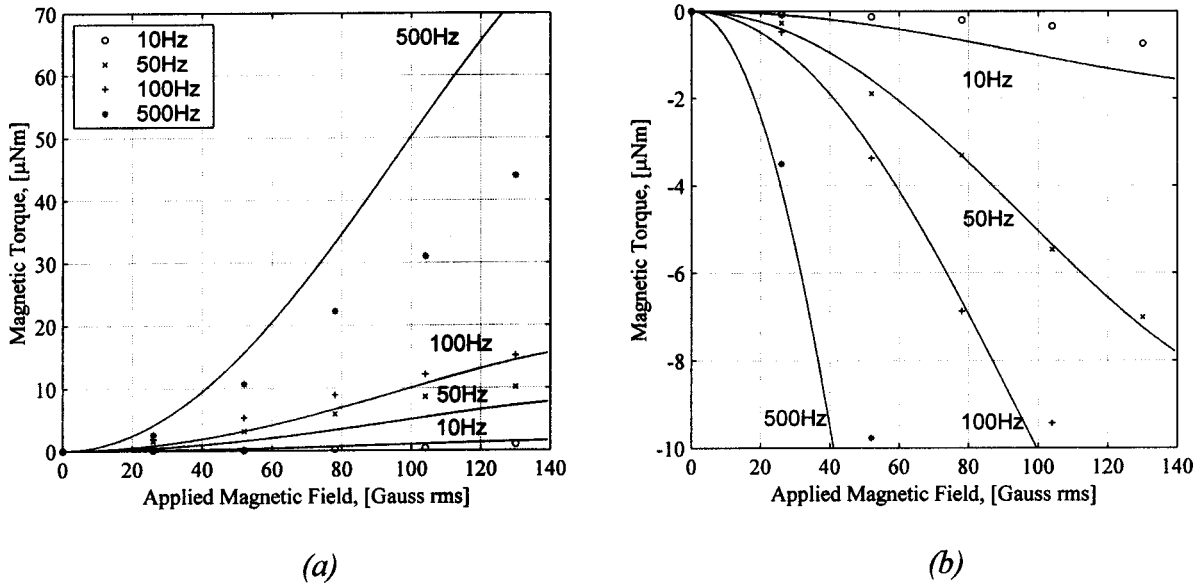

Fig. 5 Comparison between torque experimental measurements and predictions (solid lines) of (18) for the water-based ferrofluid (obtained using $\chi=0.65$, $\eta=7\times10^{-3}$ Nsm^{-2}, $\zeta=1.4\times10^{-3}$ Nsm^{-2}, $\tau=10^{-5}$ s, and $\kappa=100$). (*a*) Corresponds to clockwise rotation of the magnetic field and (*b*) corresponds to counterclockwise rotation of the magnetic field

suspension [30,31]. In vector form, the torque on a surface S relative to an arbitrary origin O, from which the position vector $\mathbf{x}$ is drawn, is given by

$$\mathbf{L}_O=\int_S \mathbf{x}\times(d\mathbf{S}\cdot\mathbf{T})+\int_S d\mathbf{S}\cdot\mathbf{C}. \tag{15}$$

The dynamical quantities $\mathbf{T}$ and $\mathbf{C}$ are functionally dependent on the gradient of the velocity field, the spin, the gradient of the spin, and a series of phenomenological material parameters, the so-called viscosities, η (shear dynamic viscosity), λ (bulk dynamic viscosity), ζ (vortex viscosity), η' (shear spin viscosity), and λ' (bulk spin viscosity)

$$\mathbf{T}=-p\mathbf{I}+\eta[\nabla\mathbf{v}+\nabla\mathbf{v}^T]+\lambda[\nabla\cdot\mathbf{v}]\mathbf{I}+\zeta\boldsymbol{\varepsilon}\cdot[\nabla\times\mathbf{v}-2\boldsymbol{\omega}], \tag{16}$$

$$\mathbf{C}=\eta'[\nabla\boldsymbol{\omega}+\nabla\boldsymbol{\omega}^T]+\lambda'[\nabla\cdot\boldsymbol{\omega}]\mathbf{I}. \tag{17}$$

Applying (15) therefore requires knowledge of the velocity, $\mathbf{v}$, and spin, $\boldsymbol{\omega}$, fields present in the flow.

A rigorous, regular perturbation analysis of the coupled ferrohydrodynamic problem corresponding to our experimental setup has been made [31], yielding $\mathbf{v}=v_\theta(r)\mathbf{i}_\theta$ and $\boldsymbol{\omega}=\omega_z(r)\mathbf{i}_z$. With these results and using (16) and (17), the axially-directed (z-directed) torque for our experimental situation is

$$L_{O,z}=-2\Omega_f\tau\chi\mu_0H^2V_f\left\{1-\frac{\tau\mu_0\chi H^2}{2\zeta}\frac{(\eta+\zeta)}{\eta^*}\frac{I_2(\kappa)}{I_0(\kappa)}\right\}, \tag{18}$$

where V_f is the volume of ferrofluid, Ω_f is the radian frequency of the magnetic field with rms amplitude H, χ is the magnetic susceptibility, ζ is the vortex viscosity, which may be estimated from [32]

$$\zeta=\frac{3}{2}\eta_0\phi_h, \tag{19}$$

where ϕ_h is the hydrodynamic volume fraction of suspended particles, η_0 is the viscosity of the suspending fluid, and η^* and κ are defined parameters, given by

$$\eta^*=\eta+\zeta\frac{I_2(\kappa)}{I_0(\kappa)}, \tag{20}$$

and

$$\kappa=\left(\frac{4\eta}{(\eta+\zeta)}\frac{R^2\zeta}{\eta'}\right)^{1/2}, \tag{21}$$

respectively. In (18) and (20), I_0 and I_2 are modified Bessel functions of the first kind and order 0 and 2, respectively. In (21), $R=9.5$ mm is the internal radius of the hollow spindle and η' is the spin viscosity of the ferrofluid. No rigorous theoretical or experimental estimates of the value of η' are currently available. Instead, η' is commonly assumed to be negligibly small, which appears plausible based on scaling arguments which assume that η' is proportional to the particle-scale dimension squared. However, we note that this is not strictly the case, as explained further in [33].

As mentioned before, a regular perturbation expansion scheme in the parameter $\Omega_f\tau$ was used to obtain these results. As such, (18) corresponds to rigorous solution of the governing fluid and magnetic field equations to second order in $\Omega_f\tau$. This regular perturbation expansion ensures that the equations of ferrohydrodynamics and Maxwell's equations [1,33] are rigorously satisfied, without neglecting the effects of spin/magnetization coupling in the magnetization relaxation equation or the demagnetizing fields. However, because of the parameter expansion in $\Omega_f\tau$, this analysis is only applicable when

$$\varepsilon\simeq\frac{\tau\mu_0\chi H^2}{2\zeta}<1. \tag{22}$$

5.3 Comparison With Experimental Observations. Figures 5 and 6 compare our experimental observations of Figs. 3 and 4 to the predictions of (18). The parameters used in obtaining Fig. 5 for the water-based ferrofluid are $\chi=0.65$, $\eta=0.007$ Nsm^{-2}, $\zeta=1.4\times10^{-3}$ Nsm^{-2} (obtained by correcting the previously obtained magnetic core volume fraction ϕ for the effect of adsorbed dispersant layers by adding 2 nm to the particle radius to account for the surfactant layer), $V_f=18.8$ cm^3, $\kappa=100$ (an *ad hoc* value, resulting in $\eta'=4.2\times10^{-11}$ Ns), and $\tau=10^{-5}$ s (adjusted to improve agreement with experimental observations). The parameters used in obtaining Fig. 6 for the Isopar-M ferrofluid are $\chi=2.2$, $\eta=0.011$ Nsm^{-2}, $\zeta=2.0\times10^{-3}$ Nsm^{-2} (again corrected for surfactant), $V_f=18.8$ cm^3, $\kappa=100$ (an *ad hoc* value, resulting in $\eta'=6.1\times10^{-11}$ Ns), and $\tau=2\times10^{-6}$ s (again adjusted to im-

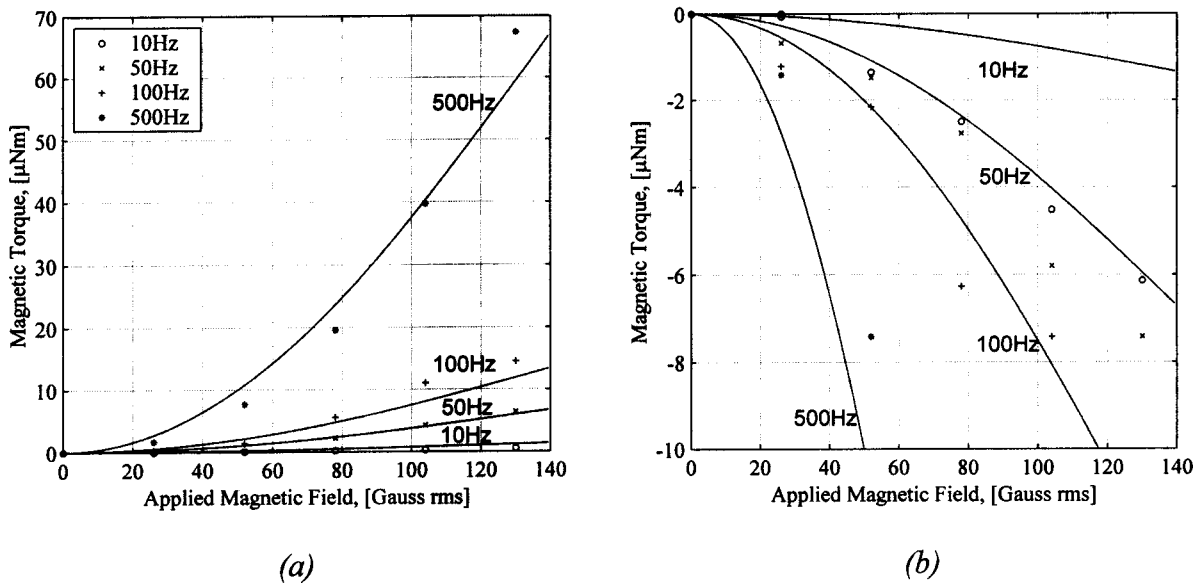

Fig. 6 Comparison between torque experimental measurements and predictions (solid lines) of (18) for the Isopar-M ferrofluid (obtained using $\chi=2.2$, $\eta=11\times10^{-3}$ Nsm^{-2}, $\zeta=2.0\times10^{-3}$ Nsm^{-2}, $\tau=2\times10^{-6}$ s, and $\kappa=100$). (*a*) Corresponds to clockwise rotation of the magnetic field and (*b*) corresponds to counterclockwise rotation of the magnetic field.

prove agreement with experimental observations). Note that for the values of $\kappa\gg1$, such as we have assumed here, we are effectively in the zero spin viscosity limit, for which (18) reduces to

$$L_{O,z}=-2\Omega_f\tau\chi\mu_0H^2V_f\left\{1-\frac{\tau\mu_0\chi H^2}{2\zeta}\right\}. \tag{23}$$

The fitted values of τ for the water-based and Isopar-M ferrofluids are in agreement with the Brownian relaxation times obtained in Section 2 (shown in Table 2), and within the calculated effective relaxation time range. This indicates that for our measurements, $\tau_N\gg\tau_B$.

Examining Figs. 5 and 6, we find reasonably good agreement between measured torques and those obtained from our theory, especially for the lower applied field frequencies. For applied field frequencies higher than 500 Hz we find poor agreement indicating perhaps other physical phenomena unaccounted for in our analysis.

Figures 5 and 6 also show low torque data (<10 μN-m) and fitted theory for counter-clockwise magnetic field rotation.

Based on the estimates provided above for the associated physical parameters in (22), we have $\varepsilon=0.35$ for the water-based ferrofluid and $\varepsilon=0.16$ for the Isopar-M ferrofluid, when the applied field strength is 140 Gauss. Higher order terms might be relevant in the analysis of the water-based ferrofluid data because of its high value of ε. The effect of higher-order terms and the analysis beyond the range specified in (22) is left to future communications.

6 Conclusions

The experiments presented herein demonstrate that even without a free surface, there is a significant torque from the viscous shear in a ferrofluid undergoing spin-up flow. Ostensibly this would result from magnetic-field-induced flow throughout the bulk of the fluid, in agreement with a recently derived analysis of the situation [31]. Our measurements show that the effect of magnetic field on torque increases with magnetic field amplitude. For most measurements, the effect on torque increases with magnetic field frequency, except for the water-based ferrofluid at frequencies greater than 500 Hz, where the torque appears to saturate.

We note that the value of ε obtained for the water-based fluid was high, indicating perhaps that higher-order terms may be necessary in analyzing experiments using the water-based ferrofluid. The large difference in τ for the two ferrofluids may also be the reason for the discrepancy. More detailed experimental and theoretical investigations, which should shed light on the observed discrepancy, are currently underway.

Although we cannot directly observe ferrofluid flow inside the opaque spindle, one could argue that the measured torque arises due to shear stresses at the fluid/spindle boundary, and hence is a result of bulk flow in the fluid. Reference [15] argues that surface stresses occurring at a ferrofluid/air interface, rather than stresses occurring throughout the volume, are responsible for magnetic-field-induced flow. Therefore, according to this presumption, in the absence of a free surface there should be no ferrofluid flow and consequently, using a stationary spindle in the viscometer setup described above, there should be no torque. The measurements presented herein show that there is indeed significant torque without a free surface and ostensibly some manner of flow arises inside the fluid.

Acknowledgments

The authors are grateful to Prof. Howard Brenner and Dr. Ronald E. Rosensweig for insightful and stimulating discussions. CR was supported in part by a Graduate Research Fellowship from the U.S. National Science Foundation. This research is supported by the U.S. National Science Foundation Grant #CTS-0084070.

References

[1] R. E. Rosensweig, 1997, *Ferrohydrodynamics*. Mineola, NY: Dover Publications.
[2] Shen, L. F., Stachowiak, A., Fateen, S. E. K., Laibinis, P. E., and Hatton, T. A., 2001, "Structure of alkanoic acid stabilized magnetic fluids. A small-angle neutron and light scattering analysis," Langmuir, **17**, pp. 288–299.
[3] Peréz-Castillejos, R., Plaza, J. A., Esteve, J., Losantos, P., Acero, M. C., Cane, C., and Serra-Mestres, F., 2000, "The use of ferrofluids in micromechanics," Sensors and Actuators A-Physical, **84**, pp. 176–180.
[4] Menz, A., Benecke, W., Pérez-Castillejos, R., Plaza, J. A., Esteve, J., Garcia, N., Higuero, J., and Diez-Caballero, T., 2000, "Fluidic components based on ferrofluids," presented at 1st Annual International IEEE-EMBS, Special Topic Conference on Microtechnologies in Medicine and Biology, Lyon, France.
[5] Hatch, A., Kamholz, A. E., Holman, G., Yager, P., and Bohringer, K. F., 2001, "A ferrofluidic magnetic micropump," J. Microelectromech. Syst., **10**, pp. 215–221.

[6] Berger, M., Castelino, J., Huang, R., Shah, M., and Austin, R. H., 2001, ''Design of a microfabricated magnetic cell separator,'' Electrophoresis, **22**, pp. 3883–3892.
[7] Zahn, M., 2001, ''Magnetic fluid and nanoparticle applications to nanotechnology,'' J. Nanoparticle Res., **3**, pp. 73–78.
[8] Roger, J., Pons, J. N., Massart, R., Halbreich, A., and Bacri, J. C., 1999, ''Some biomedical applications of ferrofluids,'' Eur. Phys. J.: Appl. Phys., **5**, pp. 321–325.
[9] Ramchand, C. N., Pande, P., Kopcansky, P., and Mehta, R. V., 2001, ''Application of magnetic fluids in medicine and biotechnology,'' Indian J. Pure Appl. Phys., **39**, pp. 683–686.
[10] Moskowitz, R., and Rosensweig, R. E., 1967, ''Nonmechanical Torque Driven Flow in Magnetic Suspensions,'' Appl. Phys. Lett., **11**, pp. 1967.
[11] Brown, R., and Horsnell, T. S., 1969, ''The wrong way round,'' Electrical Review, **183**, pp. 235.
[12] Kagan, I. Y., Rykov, V. G., and Yantovskii, E. I., 1973, ''Flow of a dielectric ferromagnetic suspension in a rotating magnetic field,'' Magnitnaya Gidrodynamika, **9**, pp. 135–137.
[13] Calugaru, G. H., Cotae, C., Badescu, R., Badescu, V., and Luca, E., 1976, ''A new aspect of the movement of ferrofluids in a rotating magnetic field,'' Reviews in Roumanian Physics, **21**, pp. 439–440.
[14] Rosensweig, R. E., and Johnston, R. J., 1989, ''Aspects of magnetic fluid flow with nonequilibrium magnetization,'' in *Continuum Mechanics and its Applications*, C. A. C. Graham and S. K. Malik, Eds.: Hemisphere Publishing Company, 1989, pp. 707–729.
[15] Rosensweig, R. E., Popplewell, J., and Johnston, R. J., 1990, ''Magnetic fluid motion in rotating field,'' Journal of Magnetism and Magnetic Materials, **85**, pp. 171–180.
[16] Zaitsev, V. M., and Shliomis, M. I., 1969, ''Entrainment of ferromagnetic suspension by a rotating field,'' J. Appl. Mech. Tech. Phys., **10**, pp. 696–700.
[17] Glazov, O. A., 1975, ''Motion of a ferrosuspension in rotating magnetic fields,'' Magnitnaya Gidrodynamika, **11**, pp. 16–22.
[18] Glazov, O. A., 1975, ''Role of higher harmonics in ferrosuspension motion in a rotating magnetic field,'' Magnitnaya Gidrodynamika, **11**, pp. 31.
[19] Glazov, O. A., 1982, ''Velocity profiles for magnetic fluids in rotating magnetic fields,'' Magnitnaya Gidrodynamika, **18**, pp. 27.
[20] Glazov, O. A., 1990, ''Dynamics of magnetic fluids in rotating magnetic fields,'' Magnitnaya Gidrodynamika, **26**, pp. 83–88.
[21] Bozorth, R. M., 1951, *Ferromagnetism*. New York, NY: IEEE Press.
[22] Shliomis, M. I., 1974, ''Magnetic fluids,'' Sov. Phys. Usp., **17**, pp. 156.
[23] Onsager, L., 1936, ''Electric Moments of Molecules in Liquids,'' J. Am. Chem. Soc., **58**, pp. 1486–1493.
[24] Shliomis, M. I., 1972, ''Effective viscosity of magnetic suspensions,'' Sov. Phys. JETP, **34**, pp. 1291–1294.
[25] Felderhof, B. U., 2000, ''Magnetoviscosity and relaxation in ferrofluids,'' Phys. Rev. E, **62**, pp. 3848–3854.
[26] Shliomis, M. I., 2001, ''Comment on Magnetoviscosity and relaxation in ferrofluids,'' Phys. Rev. E, **6406**.
[27] Felderhof, B. U., 2001, ''Reply to Comment on 'Magnetoviscosity and relaxation in ferrofluids,' '' Phys. Rev. E, **6406**.
[28] Lehlooh, A. F., Mahmood, S. H., and Williams, J. M., 2002, ''On the particle size dependence of the magnetic anisotropy energy constant,'' Physica B, **321**, pp. 159–162.
[29] Melcher, J. R., 1981, *Continuum Electromechanics*. Cambridge, MA: MIT Press.
[30] Dahler, J. S., and Scriven, L. E., 1963, ''Theory of structured continua I. General consideration of angular momentum and polarization,'' Proc. R. Soc. London, **276**, pp. 504–527.
[31] Rinaldi, C., 2002 ''Continuum Modeling of Polarizable Systems,'' Ph.D. Thesis, Massachusetts Institute of Technology, Cambridge, MA.
[32] Brenner, H., 1970, ''Rheology of two-phase systems,'' Annu. Rev. Fluid Mech., **2**, pp. 137–176.
[33] Rinaldi, C., and Zahn, M., 2002, ''Effects of spin viscosity on ferrofluid flow profiles in alternating and rotating magnetic fields,'' Phys. Fluids, **14**, pp. 2847–2870.